Dynamics and Rheology in Aqueous Solutions of Associating Diblock and Triblock Copolymers of the Same Type

Krister Thuresson,[†] Susanne Nilsson,[†] Anna-Lena Kjøniksen,[‡] Harald Walderhaug,[‡] Björn Lindman,[†] and Bo Nyström*[,‡]

Physical Chemistry 1, Chemical Center, University of Lund, P.O. Box 124, S-221 00 Lund, Sweden, and Department of Chemistry, University of Oslo, P.O. Box 1033, Blindern, N-0315 Oslo, Norway

Received: August 24, 1998; In Final Form: November 4, 1998

The associative character of monodisperse amphiphilic copolymers of the same type, one with a diblock (DB) structure (hydrophobic tail on one end) and the other with a triblock (TB) structure (hydrophobic tails on both ends), has been studied in aqueous solution. The macroscopic properties of these systems have been investigated by rheological methods and correlated to properties on the microscopic level, as revealed from pulsed field gradient NMR and dynamic light-scattering (DLS). The results suggest that, in aqueous solution, both polymers associate, but the thickening effect is much more pronounced for TB due to the gradual formation of bridges between the micellar-like clusters as the concentration increases. This connectivity effect has been surveyed by mixing the polymers in different proportions. The rheological measurements showed that the concentration induced viscosification effect is considerably stronger for TB than that for the DB system; the dynamic moduli were, even at the highest TB concentration, successfully fitted to a single Maxwell element over the experimentally accessible frequency window. The NMR self-diffusion data revealed a much stronger slowing down of the dynamics for the TB system, and a gradually broader distribution of self-diffusion coefficients was observed for this polymer as the concentration increased. The DLS results for all the solutions, except for those of the two highest TB concentrations, indicate initially an exponential decay (always diffusive) followed by a stretched exponential at longer times. For the two highest TB concentrations an additional very slow stretched exponential mode appears in the profile of the correlation function. The slow mode exhibits an approximately $\mathbf{q}^3$ ($\mathbf{q}$ is the wave vector) dependence for all the DB solutions and for the dilute TB solutions, while at higher TB concentrations this mode becomes $\mathbf{q}$ independent (the viscoelastic effect). The very slow mode shows a strong $\mathbf{q}$ dependence ($\mathbf{q}^5$). The overall picture that emerges from this study is that, at low or moderate TB concentrations and over the considered concentration range for DB, the solution consists of a collection of large clusters of various sizes, slightly interconnected to each other, while at higher TB concentrations the structure of the solution is changed to a transient network, where the connectivity is provided by bridging chains.

Introduction

Hydrophobically associating water-soluble polymers[1−13] or "associative thickeners" is a class of complex and disordered systems that have attracted a great deal of interest in recent years. These polymers are hydrophobically modified water-soluble block copolymers composed of both water-soluble and water-insoluble components (low levels of hydrophobic groups). As a result of this amphiphilic character of the polymers, they may act, even at low concentration, as powerful rheology modifiers so that they can be used in various industrial applications where the control of the rheology of the solution is required, e.g., paints, foods, pharmaceuticals, enhanced oil recovery, etc. The driving force for the association process is the interaction between the hydrophobic segments in order to minimize their exposure to water. In the very dilute concentration regime, the molecules may act as individual units, but as the concentration increases, the omnipresent hydrophobic interactions induce associations, leading to a situation where the solution contains nonaggregated species as well as clusters of various sizes and masses. At a sufficiently high concentration, a network composed of interpenetrating clusters is created. The formed associations are built up of both intra- and intermolecular contacts. The network is temporary in the sense that junctions that hold the network together break and form continuously on the time scale of experiments. Our current understanding[14−16] of networks, formed through a cluster-association process, is based on concepts such as size distribution statistics, fractal dimension, and self-similarity properties.

Dynamic light-scattering measurements on this type of systems have shown[5,12] that the decay rate of the time correlation function is slowed with increasing concentration and that the long-time behavior is described by a stretched exponential of the Kohlrausch−Williams−Watts (KWW) type. The general picture that emerges from previous studies is that the dynamics and the rheological features of these systems are complex.

Recently, well-characterized nonionic hydrophobic water-soluble diblock and triblock copolymers have been prepared. The schematic structures of the diblock and the triblock copolymers are displayed in Figure 1a. The diblock molecules (DB) are linked together two by two by reaction with isophoronediisocyanate (IPDI) to form the triblock copolymer (TB).

[†] University of Lund.
[‡] University of Oslo.

10.1021/jp983469d CCC: $18.00
Published on Web 02/11/1999

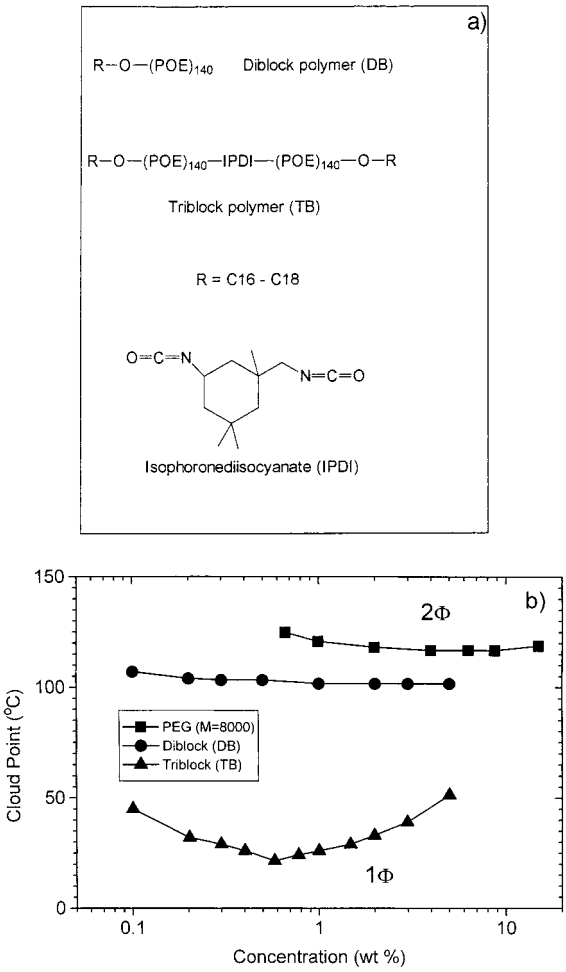

Figure 1. (a) Structure of the diblock polymer (DB) and the triblock polymer (TB). (b) Cloud point as a function of polymer concentration in aqueous solutions of DB, TB, and a poly(ethylene glycol) sample[17] with a molecular weight of 8000.

In other words, DB can be considered to have one sticker per chain, while the TB polymer has stickers on both ends of each chain. The critical micelle concentration (cmc) for the DB compound is about $10^{-7}-10^{-6}$ *m*, which indicates that this compound forms micelles at the concentrations considered in this work. Depending on the relative positions of the two hydrophobic end groups of the polymer chain, two different scenarios can be visualized.[8] Loops are formed if the end groups of the polymer are present in the same micelle. On the other hand, it is also possible that the hydrophobic end groups are located in different micelles, and in this case, a bridge is established between two micelles. The former situation is likely at low concentrations, while the latter stage is expected to be promoted at higher concentrations (cf. Figure 2 and the discussion below) for the TB polymer.

Since the diblock and triblock compounds are poly(oxyethylene)-containing polymers, we expect that solutions of these copolymers exhibit a reversed temperature dependency, i.e., phase separation takes place at elevated temperatures. The cloud point (CP) curves for the diblock and triblock copolymers, together with that of a poly(ethylene glycol) sample[17] of approximately the same molecular weight as the DB polymer, are displayed in Figure 1b. The phase behavior of the DB is similar to that for the poly(ethylene glycol) fraction. The somewhat lower values of CP for the DB sample as compared with the reference polymer can probably be ascribed to the poorer thermodynamic conditions of the system induced by the

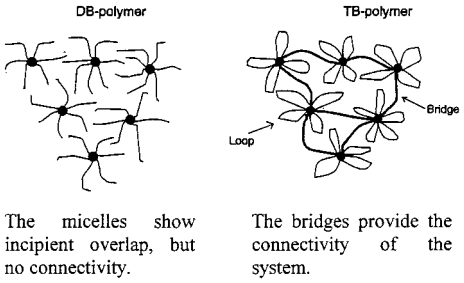

Figure 2. Schematic representation of the proposed structures of the solutions of diblock (DB) and triblock (TB) polymers.

introduction of the hydrophobic tail. More precisely, at very low concentrations the hydrophobic part may be exposed, while at higher concentrations (above cmc) the hydrophobic parts promote an association which results in an effectively higher molecular weight. Normally, an increased molecular weight of a PEG containing compound renders a lower CP.[17] In the case of the TB polymer, the values of the cloud point are located at much lower temperatures over the considered concentration range. The significant drop of CP for TB can probably to a large extent be attributed to poorer thermodynamic conditions and to the formation of flowerlike micelles connected by bridges. A special feature of systems of flower micelles composed of TB polymers is the possibility of forming bridges that give rise to a strong attraction[8,18,19] between micelles. At this state, even a moderate rise in the temperature may induce a phase separation (cf. Figure 1b) of the micelles, forming a separate phase of densely packed flowers where the neighboring micelles are connected by bridges (see Figure 2). A similar behavior with a restricted swelling of the polymer matrixes and a phase separation induced by dilution has recently been observed[20−22] in solutions of various polymers that have an attractive force between the polymer chains in common. These observations were rationalized by considering the systems as being between the two extreme cases of a solution of a flexible polymer in solution and a covalently cross-linked gel.[21] The type of associative polymers considered in this work may be modeled by a solution of molecules carrying several hydrophobic groups or stickers each. The stickers on the chains are capable of forming reversible connections by association, and this situation may involve two physical phenomena, namely, the formation of a temporary network and an increase of attraction between polymer chains induced by intermolecular associations, leading to phase separation. The effect of the connectivity results in the negative contribution to the second virial coefficient that promotes phase separation.

In a recent study[23] on the thermodymamics of aqueous mixtures of a hydrophobically modified polymer, end-capped at both ends with hydrophobic alkane groups, capable of forming associations and an unmodified polymer of the same type, the phase separation behavior was investigated. This paper indicated the importance of the entropy effect associated with the formation of junction in these systems, and it was also observed that the aggregation number of the associating polymer will affect the phase behavior.

To gain a deeper insight into the associating mechanism of these systems, rheological, pulsed field gradient NMR (PFG-NMR), and dynamic light-scattering (DLS) measurements on aqueous solutions of DB and TB and on mixtures of these copolymers have been carried out in this work. By studying different mixing ratios of TB to DB, the effect of connectivity can be modulated. The general picture that emerges from this work is that the dynamics is slowed as the concentration and

that the connectivity of the system is increased. The principal objective of this study is to elucidate the impact of concentration and connectivity on the rheological and dynamic features of associating polymers.

Experimental Section

Materials and Solution Preparation. The DB polymer has been prepared from ethoxylated, unsaturated alcohol's ($C_{16}-C_{18}$) and the "headgroup" has ca. 140 repeating EO groups. The TB polymer is synthesized in a process where two DB molecules are combined "head to head" by reaction with isophoronediisocyanate (IPDI), present in small excess, with dibutylindilaurat as a catalyst. Unreacted IPDI is eliminated by termination with small amounts of ethanol. Dilute solutions of DB and TB were dialyzed against Millipore water for several days to remove low molecular weight impurities (such as salt, oligo ethylene oxide, and IPDI terminated by ethanol) and were thereafter freeze-dried and stored in a desiccator prior to use. By using size-exclusion chromatography (SEC) (well characterized poly(ethylene glycol) fractions were used as calibration standards) the weight-average molecular weight M_w and the polydispersity index M_w/M_n were determined for both polymers. The DB sample has a M_w of 6400 and $M_w/M_n = 1.04$, and the TB sample is characterized by $M_w = 11000$ and $M_w/M_n = 1.1$.

Heavy water (Cambridge Isotope Laboratories, 99.9 atom % D) was used as a solvent in the NMR experiments to avoid disturbances caused by the water signal. To facilitate a comparison of the results obtained from the other experimental techniques, D_2O was also used in the preparation of these samples. All samples were prepared by weighing the components, and great care was exercised in the preparation procedure to obtain homogeneous solutions. All measurements were carried out on freshly prepared solutions in the concentration range 0.05−5 wt % and at a temperature of 15 °C. This low temperature was chosen to avoid complications due to phase separation phenomena.

Cloud Point Measurements. The phase separation temperatures or the cloud points (CP) of aqueous solutions of DB and TB at various concentrations were measured in glass tubes (10 mm in diameter). The temperature was changed in steps of about 1−2 °C, and the solutions were allowed to equilibrate for a few minutes before visually observing whether they had became cloudy. CP was taken as the temperature where the solutions first became hazy. Repeated runs rendered a precision of CP usually being better than ±1 °C. However, at low concentrations, and at TB concentrations around the minima in CP the uncertainty is somewhat bigger (ca. ±3 °C).

Dynamic Light Scattering. The beam from an argon ion laser (Spectra Physics model 2020), operating at 488 nm with vertically polarized light, was focused onto the sample cell through a temperature-controlled chamber (temperature controlled to within ±0.05 °C) filled with refractive index matching dibuthyl phthalate.

In light-scattering experiments we probe a wave vector $\mathbf{q} = (4\pi n/\lambda)\sin(\theta/2)$, where λ is the wavelength of the incident light in a vacuum, θ is the scattering angle, and n is the refractive index of the medium. The value of n was determined at each concentration at $\lambda = 488$ nm by using an Abbé refractometer.

In the present study the full homodyne intensity autocorrelation function $g^2(\mathbf{q},t)$ was measured at six different scattering angles in the range 30−90° with an ALV-5000 multiple τ digital correlator. The correlation functions were recorded in the real-time "multiple τ" mode of the correlator, in which 256 time channels were logarithmically spaced over an interval ranging from 0.2 μs to almost 1 h.

If the scattered field obeys Gaussian statistics, the measured correlation function $g^2(\mathbf{q},t)$ can be related to the theoretically amenable first-order electric field correlation function $g^1(\mathbf{q},t)$ by the Siegert relationship[24] $g^2(\mathbf{q},t) = 1 + B|g^1(\mathbf{q},t)|^2$, where B is usually treated as an empirical factor.

For light-scattering experiments the solutions were filtered in an atmosphere of filtered air through 0.8 μm filters (Micro Filtration Systems) directly into precleaned 10 mm NMR tubes (Wilmad Glass Company) of highest quality.

In DLS studies on associating systems[5,6,12,25−30] it has frequently been observed that the decay of the correlation function can initially be described by a single exponential, followed at longer times by a stretched exponential

$$g^1(t) = A_f \exp(-t/\tau_f) + A_s \exp[-(t/\tau_{se})^{\beta}] \qquad (1)$$

with $A_f + A_s = 1$. The parameters A_f and A_s are the amplitudes for the fast and the slow relaxation modes, respectively. When time correlation functions from DLS at long wavelengths in the semidilute regime are analyzed, the first term (short-time behavior) on the right-hand side of eq 1 yields the mutual diffusion coefficient D_m ($\tau_f^{-1} = D_m\mathbf{q}^2$), which reflects a concerted motion of polymer chains relative to the solvent. The variable τ_{se} is some effective relaxation time, and β ($0 < \beta \leq 1$) is a measure of the width of the distribution of relaxation times. The mean relaxation time is given by

$$\tau \equiv \int_0^{\infty} \exp\left[-\left(\frac{t}{\tau_{se}}\right)^{\beta}\right] dt = \frac{\tau_{se}}{\beta}\Gamma\left(\frac{1}{\beta}\right) \qquad (2)$$

where $\Gamma(1/\beta)$ is the gamma function.

In the analyzis of the present correlation function data, except for the two highest (3 and 5 wt %) TB concentrations, eq 1 was utilized and a nonlinear fitting algorithm (a modified Levenberg−Marquardt method) was employed to obtain best-fit values of the parameters. The decays of the correlation functions for the two highest concentrations of TB could not be fitted with the aid of eq 1, but an additional mode emerged in the relaxation process at very long times. This long-time tail of the correlation function, depicting the very slow dynamics of the relaxation process, could be described by another stretched exponential (the modified Levenberg−Marquardt method was also used in the fitting of this mode). This feature will be further discussed in connection with the presentation of the DLS results.

NMR Self-Diffusion Measurements. All NMR experiments were carried out in 5 mm NMR tubes with the aid of the pulsed gradient spin−echo (PGSE) NMR technique[31] on a Bruker DMX-200 spectrometer, and the polymer self-diffusion coefficients were determined. Ordinary spin−echoes ("Hahn echoes") were utilized, and the so-called preemphasis adjustment of the gradient pulses were used to avoid destabilizing effects on the echoes originating from eddy currents. The attenuation of the spin−echo amplitude after Fourier transformation was sampled as a function of the magnitude g of the applied gradient pulse ($0.5 \leq g \leq 8$ T/m).

The gradient delivery system is completely electronically controlled. The field gradients for the experimental setup with the actual probehead interface have been calibrated by the manufacturer. The calibration was checked by routine using a sample of dry glycerol at the temperature of measurement (15 °C). At various observation times Δ, and with the other parameters inside the interval used in this study, these experiments gave a diffusion coefficient that agreed with the literature

value[32] of 1.7×10^{-12} m^2 s^{-1}. The measurements were conducted by varying the magnitude of the applied magnetic field gradient g and by keeping the width of the gradient pulses δ (typically 3 ms) and Δ constant during an experiment. All measurements were performed in the narrow pulse width approximation, i.e., with $\delta \ll \Delta$. To reveal possible anomalous diffusion behavior,[33−35] experiments were carried out at different values of Δ for the highest concentrations. However, no deviation from ordinary Fick's behavior (i.e., the self-diffusion coefficient is neither time dependent nor dependent on the distance traveled by the molecules) was detected in the polymer self-diffusion measurements under the present experimental conditions.

The result of Stejskal's and Tanner's analysis[36] of the PGSE experiment is the standard equation for the spin−echo amplitude A

$$A(2\tau,g) = A_0 \exp(-2\tau/T_2) \exp[-D\gamma^2 g^2 \delta^2(\Delta - \delta/3)] \quad (3)$$

where τ is the time between the $\pi/2$ and π radio frequency pulses, T_2 is the transverse relaxation time, and γ is the magnetogyric ratio of the nucleus under consideration (the ^{1}H nucleus here). Because the experimental time Δ is kept constant during an experiment, this equation is often used in a normalized form to remove the effects of transverse relaxation

$$\Psi \equiv A(g)/A(0) = \exp[-Dk^2 t_{\text{eff}}] \quad (4)$$

where $A(g)$ and $A(0)$ are the echo amplitudes with and without the field gradient pulses, respectively, $k \equiv \gamma g \delta$ is a "generalized" scattering vector,[33,37] and $t_{\text{eff}} = \Delta - \delta/3$ is the effective experimental observation time.

In the study of hydrophobically modified polymers one usually observes that the decay of the signal intensity is nonexponential, and this behavior is probably due to effects such as polydispersity and restricted diffusion. A number of studies[5,9,10,12,35,38] on associating polymer systems have shown that the spin−echo attenuation data can be well described by a stretched exponential of the following form

$$\Psi = \exp[-(XD_{\text{se}})^{\epsilon}] \quad (5)$$

where $X = k^2 t_{\text{eff}}$, ϵ ($0 < \epsilon \leq 1$) is a measure of the width of the distribution of self-diffusion coefficients, and the quantity D_{se} is some effective self-diffusion coefficient. For a monodisperse diffusion coefficient, $\epsilon = 1$ and eq 5 reverts to eq 4. The parameter D_{se} is related to the mean self-diffusion coefficient D_s via the gamma function Γ through the expression

$$\frac{1}{D_s} = \int_0^\infty \exp[-(XD_{\text{se}})^{\epsilon}]dX = \frac{1}{\epsilon}\frac{1}{D_{\text{se}}}\Gamma\left(\frac{1}{\epsilon}\right) \quad (6)$$

The experimental NMR data were analyzed by nonlinear least-squares regression of eq 5 using the Levenberg−Marquardt algorithm. In the fitting procedure, the variables D_{se} and ϵ are treated as adjustable parameters.

There are also other methods that are capable in accounting for polydispersity effects of the system. In addition to the stretched exponential analysis, we have analyzed the spin−echo attenuation function data with the aid of the method of cumulants.[39,40] However, since the results from the two different methods are in quantitative agreement, we have chosen to only present the results from the stretched exponential approach. In this context it is interesting to note a recent study[10] on self-diffusion coefficient distributions of a hydrophobically modified polymer in aqueous solution, where the CONTIN method[41] was compared with the stretched exponential approach. The conclusion from that study was that both the CONTIN and stretched exponential analyzes fitted the spin−echo attenuation data equally well, and the position of the distribution from CONTIN was found to be in excellent agreement with the mean self-diffusion coefficient obtained from the stretched exponential analyzis.

Rheological Experiments. Oscillatory shear and viscosity measurements were conducted in a CarriMed CSL 100 constant stress rheometer, equipped with an automatic gap setting. Depending on the viscosity of the sample, a 1° acrylic cone and a plate geometry with a diameter of 4 or 6 cm, respectively, were used. The temperature was controlled to within ±0.1 °C with a Peltier plate. Before carrying out any oscillatory rheological experiments, the samples were checked to be within the linear viscoelastic region, where the storage (G') and the loss (G'') moduli are independent of the applied stress.

Results and Discussion

Before we present and discuss the results in detail it may be helpful to give some general aspects on the association process for this type of associating polymers. Since the TB polymer has two hydrophobic tails, while the DB polymer has only one, it is expected that the former is much more effective in providing the connectivity during the association process. By mixing solutions of these two polymers at different TB:DB ratios, the degree of connectivity can be modulated.

To form an effective transient network of micelles, triblock (or multiblock) copolymers with more than one collapsed block per chain are needed. At low concentrations, pairs of collapsed end blocks can stick to each other forming loops. There are essentially two factors that governs the formation of these loops, namely, the loss of the configurational entropy when the loop is formed and the energy gain due to association of collapsed blocks. As the concentration increases, the micelles overlap each other and they can reorganize into clusters of micelles connected by bridges.

The connectivity concept can be rationalized in the following scenario. A few years ago, a general theory for structural and dynamic properties of solutions of associating polymers with strongly attracting end groups was proposed.[8] In the framework of this model, it is argued that at higher concentrations a transient network of "flower" micelles, connected by multiple bridges, is formed (see Figure 2). At low TB concentrations the conjecture is that the number of bridges is small or nonexistent and that loops constitute the dominating feature. The bridges play a role of effective junction zones in the formation of the network. The development of bridges increases the configurational entropy of the middle (hydrophilic POE) blocks, but decreases the translational entropy of the micelles. As a result, the number of bridges and the size of the clusters of micelles increases with TB concentration and at a sufficiently high concentration the largest clusters of micelles connected by bridges spans across the whole solution (connectivity is established), and a network of micelles appears in the system. An important result of this approach is that bridges typically do not connect to the nearest neighbor but to distant clusters. Since the bridges can relax we have a temporary network. However, the "debridging time" is expected[8] to be very long. The essential features of this model have recently been supported[42] by numerical Monte Carlo simulations of solutions of telechelic chains with strongly attracting end groups. When it comes to the properties of solutions of the DB polymer a

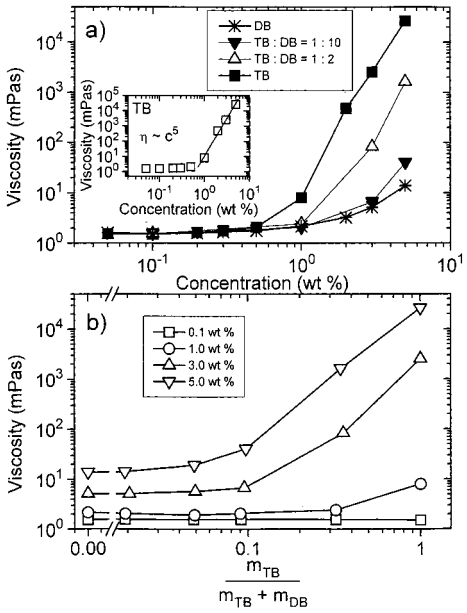

Figure 3. (a) Concentration dependence of the zero-shear viscosity for the systems indicated. The inset plot illustrates the concentration dependence of the viscosity for the TB system. (b) Effect of mixture composition on the zero-shear viscosity at the total concentrations indicated.

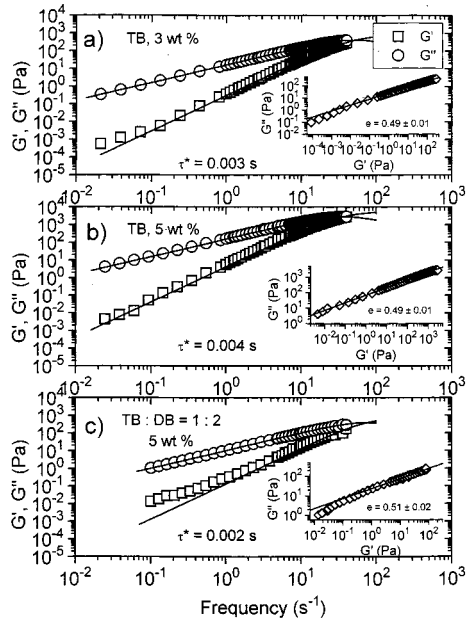

Figure 4. Storage modulus G' and loss modulus G'' as a function of frequency for the systems indicated. The solid lines represent best fits to a single Maxwell element (see eq 7). The parameter τ^* denotes the time of intersection (see text for details). The inset plots show log−log plots of G'' versus G' (see text for explanation).

different situation emerges. In this case no loops are formed because this compound is monofunctional.

Viscoelastic Properties. A conspicuous illustration of the effect of connectivity is depicted in Figure 3a, where the viscosity at low shear rate (in the zero-shear-rate Newtonian plateau) is plotted as a function of polymer concentration for DB, TB, and mixtures of these systems. A comparison of the results for DB and TB reveals that the rise in viscosity (η) occurs at a lower concentration and is much stronger for TB than that for the DB sample. Actually, the concentration dependence of the zero-shear viscosity for TB in the semidilute regime can approximately be described by a power law $\eta \sim c^x$ with $x \approx 5$ (see the plot in the inset of Figure 3a). This value of the power law exponent is the same as that observed[44,45] for solutions of flexible polymers of high molecular weight in the semidilute regime under theta solvent conditions. A stronger concentration dependence of η in the semidilute regime is usually found for flexible polymers at theta than at good solvent conditions. It has been argued[45] that the strength of entanglement coupling is higher in poor solvents than in good solvents, and this may explain the stronger concentration dependence of η at theta than at good conditions. Judging from the cloud point results of TB (see Figure 1b), this system is probably not too far from a theta-like state at the present conditions of measurement. We can see that a fairly large amount of the TB component is needed in the mixture to significantly change the concentration dependence of η from that observed in solutions with only DB (see Figure 3a). In this context we should note a recent study[20] of static and dynamic properties of a nonionic microemulsion in the presence of various amounts of hydrophobically end-capped poly(oxyethylene). The results suggest a much stronger concentration dependence of the viscosity at conditions where the system approach phase separation. This trend is compatible with the behavior depicted in Figure 3a.

The effect of composition on the viscosity is shown in Figure 3b, where η is plotted versus the ratio $m_{TB}/(m_{TB} + m_{DB})$ (m designates the weight ratio of the considered component). At the lowest concentration, η is virtually independent of the mixture ratio, while at higher total concentration the impact of the TB component on the viscosity enhancement gradually becomes stronger. The pronounced rise of the viscosity as the concentration of the TB component increases can probably be traced to an increase in the number of bridges and thereby improved connectivity.

The frequency dependences of the storage (G') and the loss (G'') modulus for the two highest TB concentrations and for a mixture of TB and DB are depicted in Figure 4. The parameter $\tau^* = 1/2\pi f^*$ is the time of intersection, or we may call it the longest relaxation time for the crossover point, and this time corresponds to the frequency of intersection f^* where G' equals G''. As indicated in Figure 4, τ^* increases with concentration of TB and it decreases when DB is added to the solution. However, the rather weak concentration dependence of τ^* at these high concentrations may suggest that the structure of the transient network does not change much. The longest relaxation time is related to the lifetime of the of the transient network.[46] However, as will be discussed below in connection with the analysis of the DLS results, τ^* is much shorter and less concentration dependent than the relaxation times determined from the long-time tails of the correlation functions from DLS for the same systems and concentrations (see, e.g., Figures 9 and 10).

The data in Figure 4 are fitted to the simplest model of a viscoelastic fluid, the Maxwell model, for which

$$G'(\omega) = G_\infty \frac{\tau^{*2}\omega^2}{1 + \tau^{*2}\omega^2}$$
$$G''(\omega) = G_\infty \frac{\tau^{*2}\omega}{1 + \tau^{*2}\omega^2} \qquad (7)$$

where G_∞ represents the plateau value of G' at high frequencies and $\omega = 2\pi f$ is the angular frequency (rad/s). As can be seen in Figure 4 (solid curves), this simple model, consisting of an elastic component (spring) connected in series with a viscous component (dashpot), describes the data quite well, thus

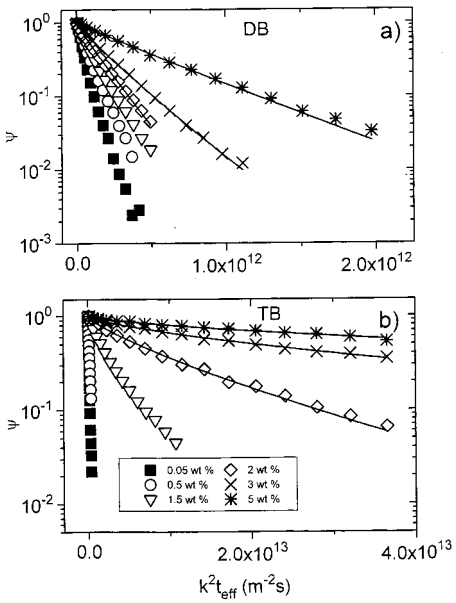

Figure 5. Plot of the proton spin−echo attenuation as a function of k^2t_{eff} for the systems and concentrations indicated. The curves are fitted with the aid of eq 5.

providing evidence that a single relaxation time controls the time scale (in this work the time window corresponds to the terminal zone of the mechanical spectrum) of the rheological properties of TB in solution. The discrepancy between the model and the experimental G'-values at low frequencies may be due to the limited resolution of the instrument.

An alternative procedure to analyze dynamic moduli data has recently been proposed.[6,47] In this approach, it was noted that if the loss modulus is plotted as a function of the storage modulus, a linear relation in a log−log plot was obtained. The value of the power law exponent e ($G'' \sim (G')^e$) is equal to 0.5 for a single Maxwell element. The results in the inset plots of Figure 4 are clearly in agreement with a simple Mawellian response. We may note that this simple behavior of a single relaxation time is in contrast to the picture that emerges from DLS, where a more complex feature appears with one or two broad relaxation modes at long times (vide infra).

Results of PGSE Experiments. Figure 5 shows plots of the normalized spin−echo attenuation as a function of the reduced variable k^2t_{eff} for aqueous solutions of DB and TB of different concentrations. The solid curves represent least-squares fits of eq 5 to the experimental data. Within the experimental errors, we observe nearly single-exponential profiles (ϵ is close to 1) of the decay functions (cf. Figure 6) for the solutions of DB in the studied concentration range, indicating a single effective rate of diffusion for all polymer molecules in the sample. However, an inspection of the spin−echo attenuation data for the solutions of TB reveals that the feature of nonexponentiality increases with increasing concentration. This behavior is illustrated in Figure 6 together with the results for mixtures of DB and TB. The general trend is that the nonexponentiality increases as the amount of the TB component becomes dominant in the mixture. It is found that a rather large amount of the TB component in a mixture of high total concentration is necessary to detect a significant feature of nonexponentiallity of the spin−echo decay. The stretched exponential character of the spin−echo attenuation can probably be associated with the formation of a network (connectivity is established) of hydrophobic clusters linked by bridging polymers at higher concentrations. At this stage, the observed diffusion units are large and the distribution

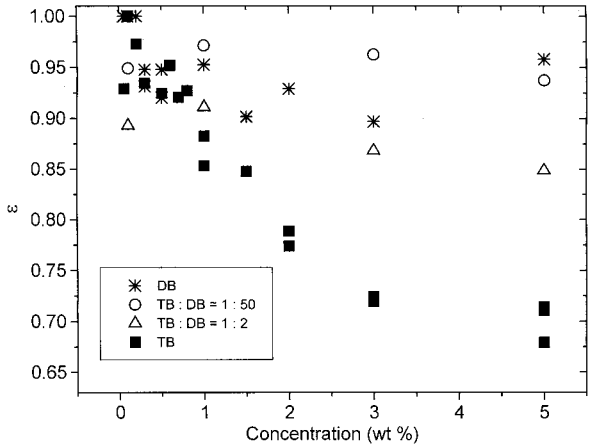

Figure 6. Concentration dependence of the width of the self-diffusion coefficient distribution (ϵ) for the systems indicated.

of cluster sizes becomes broad, giving rise to a distribution of self-diffusion coefficients. This type of behavior is manifested as a nonlinear decay in plots of the type shown in Figure 5.

It has been argued[48,49] that a universal scaling law describes the concentration and molecular weight dependence of transport properties in polymer solution. The concentration dependence of the polymer self-diffusion coefficient D_s can be described[50] by the following hydrodynamic scaling law

$$D_s(c) = D_0 \exp(-\alpha c^{\mu}) \tag{8}$$

where D_0 is the self-diffusion coefficient in the limit of infinite dilution and μ ($0.5 \leq \mu \leq 1$) and α are a scaling exponent and prefactor, respectively. This equation ascribes to D_s a stretched-exponential dependence on polymer concentration c. Phenomenologically,[48] the scaling coefficients α and μ both depend on polymer molecular weight and solvent quality.

The concentration dependence of D_s for aqueous solutions of DB and TB and for mixtures of TB and DB of different proportions is illustrated in Figure 7a, together with nonlinear least-squares fits (see the solid curves) of eq 8 to the data. The value of μ is about 0.5 for DB and approximately 1 for the TB system. Although a molecular weight dependence of μ is usually found[50] ($\mu \sim M^{-1/4}$), the detected trend cannot be explained by this effect because μ is expected to decrease with increasing molecular weight. However, if the TB system exhibits a theta-like behavior, we would expect[51] a value of μ of 1. Evidently, the concentration dependence of D_s is much stronger for the TB compound than for DB. The self-diffusion behavior observed for the TB system, as well as for other network-forming systems,[5,9,38] is typical for strongly associating systems. We may note that, for the TB system (see Figure 7a), a weaker concentration dependence of D_s is detected at the highest concentrations, which can probably be associated with enhanced topological constraints and nonuniformities of the network. In this context we may note a recent simulation study[52] on the dynamics of polymers in heterogeneous media. An interesting finding from that work is that the diffusion coefficient of a flexible macromolecule is not necessarily a monotonically decreasing function of the concentration of the medium. The results revealed a significant drop of the polymer diffusion coefficient as the concentration of obstacles of the medium increased up to a certain value, followed by rising values of the diffusion coefficient as the concentration increased further. The latter effect increases with the size of the diffusing molecules. It was argued[52] that this peculiar concentration

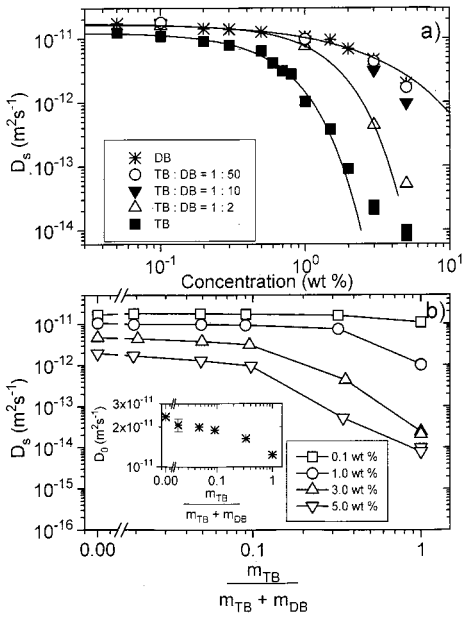

Figure 7. (a) Concentration dependence of the self-diffusion coefficient for the systems indicated. The curves are fitted with the aid of eq 8 (see text). (b) Effect of mixture composition on the self-diffusion coefficient for the total concentrations indicated. The inset plot shows how the diffusion coefficient at infinite dilution varies with the composition.

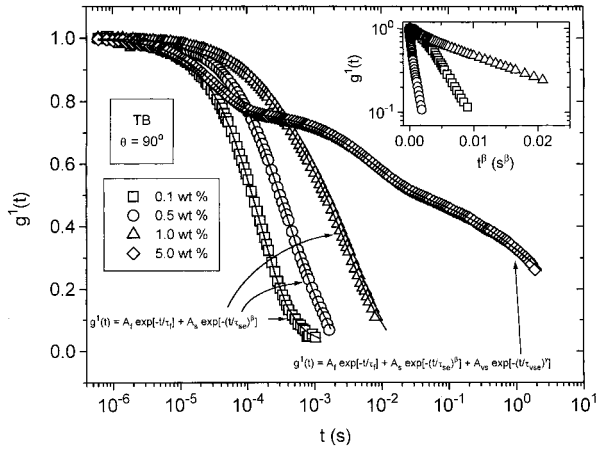

Figure 8. Plot of the first-order electric field correlation function versus time (every third data point is shown) at a scattering angle of 90° for TB at the concentrations indicated. The solid curves are fitted with the aid of the equations indicated.

dependence of the diffusion coefficient is directly related to the entropic properties[53,54] of flexible polymers in random environments and to the nature of the randomness of this environment. It is possible that enhanced nonuniformity of the network and restricted mobility of the diffusing units may be responsible for the effect detected at high concentrations of TB. However, since the hydrophobically associating TB polymer has a fairly low molecular weight and forms micelles, another scenario is possible. As the concentration increases, the micelles will gradually get into closer contact with each other and this situation facilitates a shift of the hydrophobic tails from one micelle to another. The conjecture is that this process favors the self-diffusion transport of the entities in the system.

The results in Figure 7a reveal a stronger concentration dependence of D_s as the amount of the TB component in the mixture of TB and DB increases. We can see that 10% (of the dry weight) or more of the TB component in the mixture is needed to reveal a significant change of the concentration dependence of D_s from that of the pure DB system. The effect of the ratio TB:DB on the diffusion behavior at various total concentrations of the mixture is depicted in Figure 7b. These results show that the self-diffusion coefficient falls off as the amount of the TB component rises, and this tendency becomes gradually more marked as the total concentration of the mixture increases. It is obvious from these findings that the contribution from the TB component is of vital importance for the substantial slowing down of the chain motion observed in mixtures of high total concentration. The inset plot shows how the diffusion coefficient at infinite dilution D_0 changes with the composition of the system. The value of D_0 drops as the amount of the TB component increases. It is possible that this tendency reflects the fact that the molecular weight of the TB polymer is approximately twice as high as that of DB. However, since the slow mode is present in the profile of the correlation function from DLS even at very low concentrations (see below), an incipient formation of aggregates of TB cannot be excluded and this effect may contribute to the observed decrease of D_0.

Dynamic Light Scattering. The decay of the time correlation function can for all the solutions, except for the two highest concentrations (3 and 5 wt %) of the aqueous TB system, be described by eq 1. The change in behavior is illustrated in Figure 8, which shows time correlation function data (at a scattering angle of 90°) for TB solutions of various concentrations. The correlation functions representing the three lowest concentrations have been fitted with the aid of eq 1 (solid curves). The inset shows semilogarithmic plots of $g^1(t)$ data as a function of t^β for the concentrations indicated. This type of plot yields straight lines for functions that can be portrayed by stretched exponentials. We observe that the long-time behavior is well described by straight lines for the considered concentrations. The value of the stretched exponent is in the approximate range 0.7−0.9 for both DB and TB and it is practically independent of concentration, composition of the mixture, and the scattering angle. At the two highest TB concentrations (3 and 5 wt %), the decay of the correlation function exhibits a more complex behavior. In this case, a third mode, which also shows a stretched exponential character, appears in the profile of the correlation function at very long times (see Figure 8). The width of the distribution of relaxation times is broader (the value of the stretched exponential γ is about 0.4) than for the intermediate mode ($\beta = 0.7-0.9$). At high concentrations, we have probably a network formed by interconnected clusters. This will be discussed in more detail below.

Figure 9 shows a comparison of the correlation functions (at a scattering angle of 30°) for DB and TB solutions of different concentration. The results clearly reveal that there is, especially for the two highest concentrations, a much stronger shift in the decay time toward higher values for TB than for DB. The pronounced slowing down of the relaxation process observed at higher TB concentrations can probably be attributed to the network connectivity and the long "debridging time" at these conditions. A characteristic feature of both systems is the plateaulike region of the correlation function at intermediate times for the two highest concentrations. This behavior indicates formation of large clusters,[55,56] and the plateaulike region is more prominent at low scattering angles (cf. Figures 8 and 9). Similar findings have been reported[6,28,55−58] for other associating polymer systems.

The effect of mixture composition on the decay of the correlation function is displayed in Figure 10 for a constant concentration of 3 wt %. At low and moderate amounts of TB in the mixture, the correlation functions can virtually be

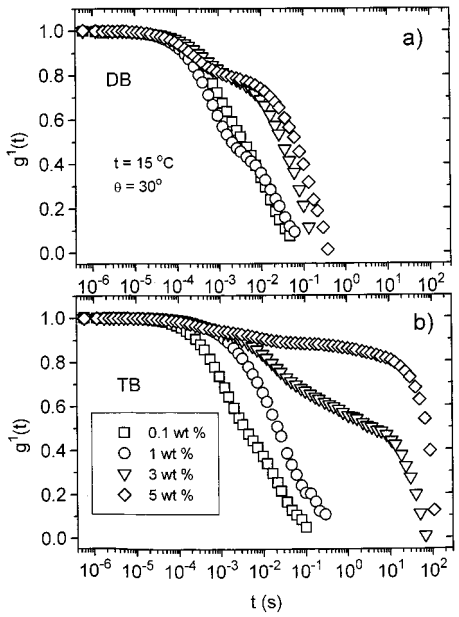

Figure 9. Plot of the first-order electric field correlation function versus time (every third data point is shown) at a scattering angle of 30° for the systems and concentrations indicated.

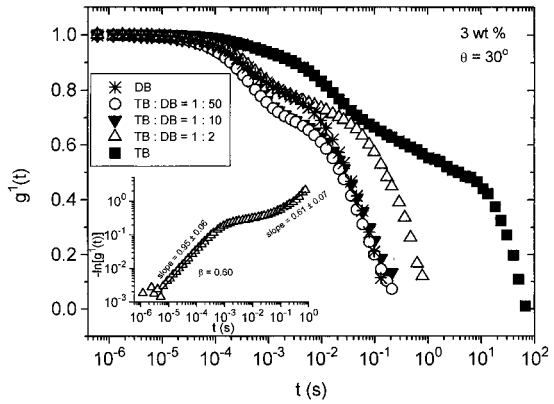

Figure 10. Plot of the first-order electric field correlation function versus time (every third data point is shown) at a scattering angle of 30° and at a fixed concentration of 3 wt % for the systems indicated. The inset plot shows an illustration of $\log(-\ln(g^1(t)))$ against $\log(t)$ for a mixture with a TB to DB ratio of 1:2. See text for details.

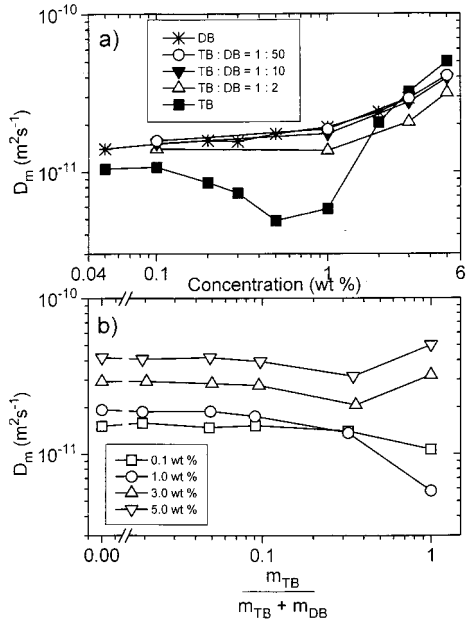

Figure 11. (a) Concentration dependence of the mutual diffusion coefficient for the systems indicated. (b) Effect of mixture composition on the mutual diffusion coefficient at the total concentrations indicated.

superimposed on that representing the pure DB system. However, at a TB to DB ratio of 1:2, we observe a marked shift in the relaxation time toward longer times. These results suggest that a fairly large amount of the TB component in the mixture is required to cause an enhanced slowing down of the long-time relaxation process.

A conspicuous illustration of the short time and long time behavior of the dynamics for a mixture with a TB to DB ratio of 1:2 is displayed in the inset plot of Figure 10, where a plot of the form $\log(-\ln(g^1(t)))$ versus $\log t$ is shown. This type of plot has recently[59] been utilized in the analysis of short and long time relaxation effects of correlation functions of concentrated colloid suspensions. In this approach, the fast relaxation process is characterized by a straight line with a slope equal to one, and the slow mode yields a slope that equals the value of the stretched exponent β. This type of plot facilitates the observation of crossover effects in the profile of the correlation function.

Let us first discuss the features of the fast relaxation mode, which is observed to be $\mathbf{q}^2$ dependent for all the systems and is therefore diffusive. It is well-known that the mutual diffusion process of polymer systems is governed by the interplay between hydrodynamic and thermodynamic properties through the relationship[60] $D_m \cong s\partial\Pi/\partial c$, where s is the sedimentation coefficient and $\partial\Pi/\partial c$ is the inverse osmotic compressibility. In general, the sedimentation coefficient (the hydrodynamic factor) falls off with increasing concentration, whereas the thermodynamic factor $\partial\Pi/\partial$c rises as the concentration increases. At good and moderately good thermodynamic conditions, $\partial\Pi/\partial c$ dominates and D_m is expected to increase with concentration. At conditions close to or at the theta temperature, a more complex concentration dependence of the mutual diffusion coefficient can be anticipated. In this case the hydrodynamic factor dominates at low concentrations, while the thermodynamic factor reigns in the semidilute regime. As a result, D_m will pass through a minimum[61−63] as the concentration increases.

The concentration dependence of the mutual diffusion coefficient (calculated from the fast relaxation mode) at different ratios of mixture is shown in Figure 11a. For the DB system and for mixtures with low or moderate amounts of TB, D_m increases with increasing concentration in a way that is typical for polymer solutions at good or moderately good thermodynamic conditions.[62,63] For the TB system, on the other hand, a quite different diffusion behavior is observed. In this case the diffusion coefficient passes through a minimum and the concentration dependence of D_m in the semidilute regime can approximately be described by the power law $D_m \sim c^1$. This power law is predicted[64] for flexible high polymers in the semidilute regime at theta solvent conditions. A number of experimental diffusion studies[63,65] of semidilute polystyrene solutions at the theta temperature support this theoretical prediction. In light of this we may argue that in this concentration range the present TB system exhibits a theta-like diffusion behavior. The effect of composition of the mixture on the diffusion process at different total concentrations is illustrated in Figure 11b. The diffusion coefficient is practically independent of the mixture ratio, except in the limit of the pure TB component where D_m drops at low concentrations and increases at high total concentration. This trend can be traced to the concentration dependence of D_m for the TB component.

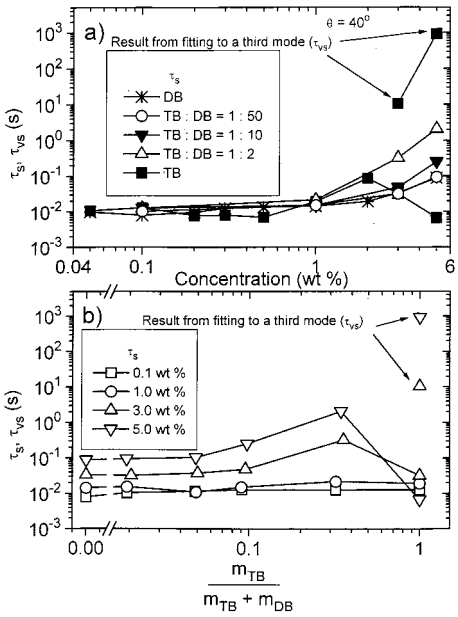

Figure 12. (a) Concentration dependence of the slow (τ_s) and very slow (τ_{vs}) relaxation time at a scattering angle of 40° for the systems indicated. (b) Effect of mixture composition on the slow (τ_s) and very slow (τ_{vs}) relaxation time at the total concentrations indicated.

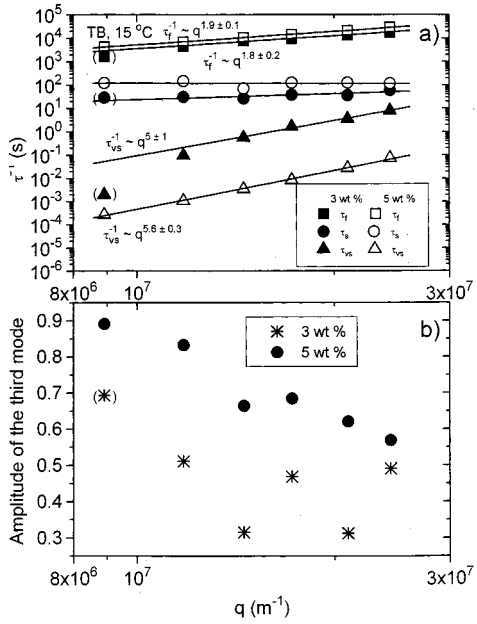

Figure 13. (a) Inverse relaxation times as a function of the wave vector for TB at the concentrations indicated. (b)Wave vector dependence of the third amplitude for TB at the concentrations indicated (see text).

In Figure 12a, the concentration dependence of the slow relaxation time at different TB:DB ratios is shown. The general trend is that τ_s rises with increasing concentration and that this feature is more pronounced as the amount of TB increases in the mixture. However, the peculiar decrease of τ_s observed for the two highest TB concentrations can probably be attributed to crossover effects in connection with the transition from the slow mode to the very slow mode (or the ultraslow mode), represented by the long-time tail of the correlation function. We can see that the relaxation times for the very slow mode are extremely long (cf. Figures 8 and 9b). This behavior is expected because the "debridging" time or the time for cluster disengagement relaxation should increase as the TB content of the mixture grows and the connectivity of the network is strengthened. A further illustration of this effect is depicted in Figure 12b, where τ_s is plotted versus the composition of the mixture. Again the strong influence of the TB component in TB−DB mixtures on the relaxation process is demonstrated. At low concentrations, the slow relaxation time is virtually unaffected by the composition of the mixture, while at higher concentrations the dynamics is considerably slowed as the amount of TB in the mixture increases. Again we have evidence that the TB polymer plays a crucial role in the establishment of a strong network at higher concentrations.

The **q** dependences of the inverse fast, slow, and very slow relaxation times may be expressed as $\tau_f^{-1} \sim \mathbf{q}^{\alpha}$f, $\tau_s^{-1} \sim \mathbf{q}^{\alpha}$s, and $\tau_{vs}^{-1} \sim \mathbf{q}^{\alpha}$vs, respectively. To quantitatively determine the angular dependences of the three different relaxation modes, plots of the inverse relaxation times as a function of **q** have been constructed for the two highest TB concentrations (see Figure 13a). Within experimental errors, α_f, always assume a value of 2, which is the hallmark of a diffusive process.

Figure 14 shows the effects of concentration and composition on the **q** dependences of the slow and very slow relaxation modes. Except for TB solutions of high concentration, the slow mode exhibits a somewhat stronger **q** dependence than the diffusive process. This **q** dependency indicates internal motions with strong hydrodynamic interactions (Zimm-like behavior) and may be interpreted as arising from large clusters of various sizes

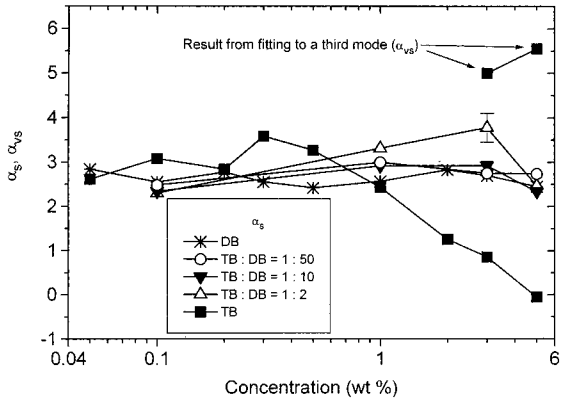

Figure 14. Power law exponent, illustrating the **q** dependence of the slow (τ_s) and ultraslow (τ_{vs}) relaxation times, as a function of concentration for the systems indicated (see text).

or the presence of large-scale "heterogeneities".[55,66,67] A number of DLS studies[5,6,25,29,30,58,68] on associating polymer systems and gelling systems have revealed that the **q** dependence of the slow mode is stronger than that of the fast mode.

When it comes to the **q** dependence of the slow relaxation mode for the TB system, a more complex picture emerges. In this case a stronger **q** dependence of the slow mode than that of a diffusive process is found at low concentrations, but as the concentration increases the value of α_s decreases and the slow mode becomes virtually **q** independent at high concentrations. This type of drop in the power law exponent α_s as the viscoelastic properties of the system evolve has recently been reported for associating[69,70] and gelling[29] systems. As will be discussed below, our surmise is that the **q** independent mode is of structural origin and due to the enhanced viscoelasticity of the transient physical network, formed as a result of the bridging process.

A **q** independent slow mode was originally observed[65,71,72] for semidilute solutions of flexible polymers (e.g., polystyrene) at theta solvent conditions. However, this feature has also been reported[29,69,70] for associating and gelling polymer systems at nontheta solvent conditions and for entangled[73] solutions of

flexible polymers at good solvent conditions. There are several theoretical approaches[65,71,74−78] that have addressed the **q** independent slow mode through the coupling of the concentration fluctuation and the viscoelastic effect. The model of Wang[76] predicts that the slow mode, characterizing the structural or viscoelastic mode, consists of a distribution of relaxation times that are all independent of **q** because the viscoelastic response is not of hydrodynamic origin. In view of these considerations, the **q** dependence of the slow mode for the present systems may be rationalized in the following way. At low TB concentrations and at all concentrations considered for the other systems, the solutions consist of nonentangled clusters of various sizes and the relaxation process is relatively fast. At higher TB concentrations, the connectivity of the network is gradually established and the system exhibits an enhanced viscoelastic response and a long debridging time.

The **q** dependence of the very slow or ultraslow relaxation mode (the long-time tail of the correlation function), observed for TB solutions of 3 and 5 wt %, is strong with a value of α_{vs} of approximately 5 (see Figure 14). This behavior is probably associated with internal dynamics of very large clusters formed during the debridging process. The fact that the amplitude of the third mode strongly depends on q, increasing with decreasing scattering angle (see Figure 13b), suggests scattering by large moieties. In a recent DLS study[79] on diblock copolymer solutions, a very slow diffusive relaxation mode was detected, which was attributed to "long-range density fluctuations" or the relaxation of the clusters formed by the copolymer molecules. This type of behavior has also been reported for diblock copolymer melts[80−82] and for semidilute diblock copolymer solutions.[83,84] In this context it is interesting that, in a recent study[70] of the dynamic properties of solutions of telechelic ionomers, a third very slow mode was observed in the profile of the correlation function at high concentrations. This mode was reported to exhibit a strong **q** dependence and the origin of this relaxation mode was attributed to large scale inhomogeneities in the viscous samples.

The strong angular dependence of the very slow inverse relaxation time may be rationalized in the phenomenological coupling model of Ngai,[85,86] dealing with the problem of how the relaxation of a specific chain or cluster is slowed due to the coupling to complex surroundings. This coupling model predicts[85] that $\alpha_{vs} = 2/\gamma$. Since the value of the stretched exponent γ for the very slow mode is close to 0.4, this approach yields a value that is consistent with the observed **q** dependence of the very slow mode.

Before we end this section it may be fruitful to compare features that have bearing on both rheology and DLS. The results from the present reological measurements, which cover the terminal zone of the mechanical spectrum, are well described by a Maxwellian response, suggesting a single relaxation process. Rheological studies of systems such as telechelic HEUR (hydrophobic ethoxylated urethane) associative polymers,[23,87−90] both monodisperse and polydisperse samples, different telechelic ionomers,[70,91] and semidilute aqueous solutions of poly(vinyl alcohol)[69] in the presence of sodium borate have all shown that the viscoelastic properties can be described in terms of the single element Maxwell model. These results indicate that the relaxation process of these systems is dominated by a single terminal relaxation time. It has been argued[87] that this relaxation time depends primarily on the hydrophobe chain length but also to a lesser extent upon polymer concentration and the molecular weight of the polymer. In studies[5,69,70] where also DLS measurements have been carried out, a more complex time dependence of the relaxation function is observed. In this case the decay of the correlation function can be described by a fast relaxation mode at short times, which displays a single exponential profile, followed by one or two slow modes at longer times. The latter modes are usually characterized by a broad distribution of relaxation times. The viscoelastic properties probed in rheology are akin to the slow mode in DLS that is **q** independent. For the TB solutions of the two highest concentrations such a mode was observed with a broader distribution of relaxation times than the rheological counterpart. A similar behavior has recently been reported[70] from a study of telechelic ionomers.

Above we have discussed systems where the viscoelastic response probed from rheology can be described by a single Maxwell element. However, we should note that there are several rheological investigations in the literature that has reported a significant departure from a single Maxwell element. Typical systems that belong to this category are: semidilute aqueous solutions of unmodified[6,47,89] ethyl(hydroxyethyl)-cellulose (EHEC) and hydrophobically modified EHEC,[6,47] solutions of a poly(ethylene oxide)−poly(propylene oxide)−poly(ethylene oxide) triblock copolymer,[92] and semidilute aqueous solutions of hydrophobically modified polyacrylamide.[93] These results indicate that the time evolution of the relaxation following a perturbation is highly nonexponential and that the relaxation processes in all of these systems are characterized by the broad distributions of the relaxation times. In a recent Monte Carlo study[94] of relaxation dynamics of transient networks formed by triblock copolymers, it was found that the stress relaxation function exhibits a nonexponential decay in such systems. It was argued that the nonexponentiality in this function is a consequence of the polydispersity in the micelles as well as the existence of more than one relaxation pathway. On the basis of these results, it seems likely that the shape of the profile of the relaxation function depends on the topology of the transient network.

Another finding of this work that deserves attention is the fact that the long time cutoff of the DLS relaxation function is always significantly higher than the longest relaxation time from rheology. This observation is consistent with the behavior reported from studies of telechelic ionomers[70] and triblock copolymers in solvents selective for the center block.[95,96] These results indicate that concentration fluctuations take a longer time to relax than shear stress. If the decay of the correlation function is interpreted in terms of cooperative diffusion and longitudinal stress relaxation modes, a simplified approach of existing theoretical models yields[70] a **q** independent slow relaxation time that is related to the longest relaxation time τ^* through $\tau_s = \tau^*(M_0/K_{os})$, where M_0 ($M_0 = K_{os} + 4G_0/3$; G_0 is the shear modulus) is the longitudinal gel modulus and K_{os} is the osmotic modulus. In this framework, the present results imply that M_0 is much larger than K_{os} and that the DLS experiments are more sensitive to shear relaxation than osmotic relaxation. The observation that the **q** independent relaxation time τ_s is larger than τ^* and with a broader distribution of times is consistent with a picture where the relaxation is due to restructuring of small scale inhomogeneities. However, we should bear in mind that it is also possible that oscillatory shear perturbations may be conducive to the difference between the longest relaxation time and the characteristic relaxation times from DLS if they can promote a faster cluster disengagement relaxation.

Conclusions

We have examined the association behavior of monodisperse amphiphilic copolymers of two types—one is a diblock copoly-

mer (DB) (containing one hydrophobic tail per chain) and the other is a triblock copolymer (TB) (containing two hydrophobic tails per chain)—in aqueous solution by using different experimental techniques. Both polymers seem to form micelle-like aggregates at elevated concentration, but the association structures of the systems are quite different. The results indicate that the DB solutions consist of individual entities, or at higher concentrations, slightly interconnected clusters of various sizes, while the TB system forms a transient network of micelles connected by bridges at higher concentrations.

The dynamic moduli, recorded in the terminal zone of the mechanical spectrum, can be fitted to a single Maxwell element which suggests that the rheological features are fairly simple and the relaxation process can be characterized by a single exponential relaxation time. When it comes to the DLS results a more intricate picture emerges. In this case the decay of the correlation function can be described by a single exponential at short time (diffusive mode), followed by a stretched exponential at long times. However, for the two highest TB concentrations an additional very slow relaxation mode appears in the profile of the correlation function. We have found that the slow mode is approximately $\mathbf{q}^3$ dependent for aqueous solutions of DB over the considered concentration range and for low concentrations of TB. This behavior indicates the formation of large clusters. At high TB concentrations, the slow mode becomes **q** independent, suggesting that this mode is of structural origin and due to the enhanced viscoelasticity of the transient physical network, formed by bridging micelles. The existence of the very slow relaxation mode and its strong **q** dependence ($\mathbf{q}^5$) indicate that the "debridging time" is very long and that large clusters or large scale inhomogeneities are formed during the debridging process.

Acknowledgment. We thank Akzo Nobel Surface Chemistry AB for supplying the polymer samples. K.T. and S.N. thank the Centre for Amphiphilic Polymers (CAP) for financial support. The rheometer was funded by a grant from Nils and Dorthi Troëdsson's Research Foundation.

References and Notes

(1) McCormick, C. L.; Bock, J.; Schulz, D. N. In *Encycl. of Polym. Sci. Eng.* **1989**, *17*, 730.
(2) Glass, J. E., Ed. *Polymers in Aqueous Media*; Advances in Chemistry Series 223; American Chemical Society: Washington, DC, 1989.
(3) Wang, Y.; Winnik, M. A. *Langmuir* **1990**, *6*, 1437.
(4) Seery, T. A. P.; Yassini, M.; Hogen-Esch, T. E.; Amis, E. J. *Macromolecules* **1992**, *25*, 4784.
(5) Nyström, B.; Walderhaug, H.; Hansen, F. K. *J. Phys. Chem.* **1993**, *97*, 7743.
(6) Nyström, B.; Thuresson, K.; Lindman, B. *Langmuir* **1995**, *11*, 1994.
(7) Yekta, A.; Xu, B.; Duhamel, J.; Adiwidjaja, H.; Winnik, M. A. *Macromolecules* **1995**, *28*, 956.
(8) Semenov, A. N.; Joanny, J.-F.; Khokhlov, A. R. *Macromolecules* **1995**, *28*, 1066.
(9) Rao, B.; Uemura, Y.; Dyke, L.; Macdonald, P. M. *Macromolecules* **1995**, *28*, 531.
(10) Persson, K.; Griffiths, P. C.; Stilbs, P. *Polymer* **1996**, *37*, 253.
(11) Sun, T.; Jr., King, H. E. *Macromolecules* **1996**, *29*, 3175.
(12) Walderhaug, H.; Nyström, B. *Trends Phys. Chem.* **1997**, *6*, 89.
(13) Chassenieux, C.; Nicolai, T.; Durand, D. *Macromolecules* **1997**, *30*, 4952.
(14) Daoud, M.; Martin, J. E. In *The Fractal Approach to Heterogeneous Chemistry*; Avnir; D., Ed.; John Wiley & Sons: New York, 1989.
(15) Dusek, K. *Recl. Trav. Chim. Pays-Bas* **1991**, *110*, 507.
(16) Sahimi, M. *Mod. Phys. Lett. B* **1992**, *6*, 507.
(17) Saeki, S.; Kuwahara, N.; Nakata, M.; Kaneko, M. *Polymer* **1976**, *17*, 685.
(18) Witten, T. A. *J. Phys.* **1988**, *49*, 1055.
(19) Milner, S. T.; Witten, T. A. *Macromolecules* **1992**, *25*, 5495.
(20) Bagger-Jörgensen, H.; Coppola, L.; Thuresson, K.; Olsson, U.; Mortensen, K. *Langmuir* **1997**, *13*, 4204.
(21) Thuresson, K.; Joabsson, F. *Colloids. Surf.* 1999. In press.
(22) Thuresson, K.; Piculell, L.; Lindman, B. *J. Dispersion Sci. Technol*. 1999. In press.
(23) Annable, T.; Ettelaie, R. *Macromolecules* **1994**, *27*, 5616.
(24) Siegert, A. J. F. Radiation Laboratory Report No. 465; Massachusetts Institute of Technology: Cambridge, 1943.
(25) Nyström, B.; Roots, J.; Carlsson, A.; Lindman, B. *Polymer* **1992**, *33*, 2875.
(26) Martin, J. E.; Adolf, D. *Annu. Rev. Phys. Chem.* **1991**, *42*, 311.
(27) Lang, P.; Burchard, W. *Macromolecules* **1991**, *24*, 814.
(28) Hodgson, D. F.; Yu, Q.; Amis, E. J. In *Synthesis, Characterization, and Theory of Polymeric Networks and Gels*; Aharoni, S. M., Ed.; Plenum Press: New York, 1992.
(29) Nyström, B.; Lindman, B. *Macromolecules* **1995**, *28*, 967.
(30) Konak, C.; Helmstedt, M.; Bansil, R. *Macromolecules* **1997**, *30*, 4342.
(31) Stilbs, P. *Prog. Nucl. Magn. Reson. Spectrosc.* **1987**, *19*, 1.
(32) Hrovat, M. I.; Wade, C. G. *J. Magn. Reson*. **1981**, *44*, 62.
(33) Callaghan, P. T. *Principles of Nuclear Magnetic Resonance Microscopy*; Oxford University Press: New York, 1991.
(34) Gefen, Y.; Aharony, A.; Alexander, S. *Phys. Rev. Lett.* **1983**, *50*, 77.
(35) Walderhaug, H.; Nyström, B. *J. Phys. Chem. B* **1997**, *101*, 1524.
(36) Tanner, J. E.; Stejskal, E. O. *J. Chem. Phys.* **1968**, *49*, 1768.
(37) Fleischer, G.; Fujara, F. *NMR* **1994**, *30*, 159.
(38) Abrahmsén-Alami, S.; Stilbs, P. *J. Phys. Chem.* **1994**, *98*, 6359.
(39) Koppel, D. E. *J. Chem. Phys.* **1972**, *57*, 4814.
(40) Callaghan, P. T.; Pinder, D. N. *Macromolecules* **1983**, *16*, 968.
(41) Provencer, S. W. *Comput. Phys. Commun.* **1982**, *27*, 213, 229.
(42) Khalatur, P. G.; Khokhlov, A. R. *Macromol. Theory Simul.* **1996**, *5*, 877.
(43) Adam, M.; Delsanti, M. *J. Phys. (Paris)* **1982**, *43*, 549.
(44) Adam, M.; Delsanti, M. *J. Phys. (Paris)* **1984**, *45*, 1513.
(45) Takahashi, Y.; Isono, Y.; Noda, I.; Nagasawa, M. *Macromolecules* **1985**, *18*, 1002.
(46) Rubinstein, M.; Dobrynin, A. V. *Trends Polym. Sci.* **1987**, *5*, 181.
(47) Thuresson, K.; Lindman, B.; Nyström, B. *J. Phys. Chem. B* **1997**, *101*, 6450.
(48) Phillies, G. D. J. *J. Phys. Chem*. **1989**, *93*, 5029.
(49) Phillies, G. D. J. *Macromolecules* **1998**, *31*, 2317.
(50) Phillies, G. D. J. *Macromolecules* **1986**, *19*, 2367.
(51) Phillies, G. D. J.; Clomenil, D. *Macromolecules* **1993**, *26*, 167.
(52) Slater, G. W.; Wu, S.-Y. *Phys. Rev. Lett.* **1995**, *75*, 164.
(53) Baumgärtner, A.; Muthukumar, M. *J. Chem. Phys.* **1987**, *87*, 3082.
(54) Muthukumar, M.; Baumgärtner, A. *Macromolecules* **1989**, *22*, 1941.
(55) Richtering, W.; Löffler, R.; Burchard, W. *Macromolecules* **1992**, *25*, 3642.
(56) Richtering, W.; Gleim, W.; Burchard, W. *Macromolecules* **1992**, *25*, 3795.
(57) Smits, R. G.; Kuil, M. E.; Mandel, M. *Macromolecules* **1994**, *27*, 5599.
(58) Kjøniksen, A.-L.; Nyström, B. *Macromolecules* **1996**, *29*, 7116.
(59) Ngai, K. L.; Rendell, R. W. *Philos. Mag. B* **1998**, *77*, 621.
(60) De Gennes, P.-G. *Scaling Concepts in Polymer Physics*; Cornell University Press: Ithaca, NY, 1979.
(61) Rehage, G.; Ernst, O.; Fuhrmann, J. *Discuss. Faraday Soc.* **1970**, *49*, 208.
(62) Roots, J.; Nyström, B.; Sundelöf, L.-O.; Porsch, B. *Polymer* **1979**, *20*, 337.
(63) Roots, J.; Nyström, B. *Macromolecules* **1980**, *13*, 1595.
(64) Brochard, F.; de Gennes, P.-G. *Macromolecules* **1977**, *10*, 1157.
(65) Adam, M.; Delsanti, M. *Macromolecules* **1985**, *18*, 1760.
(66) Koberstein, J. T.; Picot, C.; Benoit, H. *Polymer* **1985**, *28*, 673.
(67) Bodycomb, J.; Hara, M. *Macromolecules* **1995**, *28*, 8190.
(68) Ren, S. Z.; Sorensen, C. M. *Phys. Rev. Lett*. **1993**, *70*, 1727.
(69) Koike, A.; Nemoto, N.; Inoue, T.; Osaki, K. *Macromolecules* **1995**, *28*, 2339.
(70) Johannsson, R.; Chassenieux, C.; Durand, D.; Nicolai, T.; Vanhoorne, P.; Jérôme, R. *Macromolecules* **1995**, *28*, 8504.
(71) Brochard, F. *J. Phys. (Paris)* **1983**, *44*, 39.
(72) Stepanek, P.; Konak, C.; Jakes, J. *Polym. Bulletin* **1986**, *16*, 67.
(73) Jian, T.; Vlassopoulos, D.; Fytas, G.; Pakula, T.; Brown, W. *Colloid Polym. Sci.* **1996**, *274*, 1033.
(74) Brochard, F.; de Gennes, P.-G. *Macromolecules* **1977**, *10*, 1157.
(75) Semenov, A. N. *Physica A* **1990**, *166*, 263.
(76) Wang, C. H. *J. Chem. Phys.* **1991**, *95*, 3788.; *Macromolecules* **1992**, *25*, 1524.
(77) Doi, M.; Onuki, A. *J. Phys. II Fr.* **1992**, *2*, 1631.
(78) Genz, U. *Macromolecules* **1994**, *27*, 3501.
(79) Jian, T.; Anastasiadis, S. H.; Semenov, A. N.; Fytas, G.; Adachi, K.; Kotaka, T. *Macromolecules* **1994**, *27*, 4762.
(80) Vogt, S.; Jian, T.; Anastasiadis, S. H.; Fytas, G.; Fischer, E. W. *Macromolecules* **1993**, *26*, 3357.

(81) Anastasiadis, S. H.; Fytas, G.; Vogt, S.; Fischer, E. W. *Phys. Rev. Lett.* **1993**, *70*, 2415.
(82) Anastasiadis, S. H.; Fytas, G.; Vogt, S.; Gerharz, B.; Fischer, E. W. *Europhys. Lett.* **1993**, *22*, 619.
(83) Haida, H.; Lingelser, J.P.; Gallot, Y.; Duval, M. *Makromol. Chem.* **1991**, *192*, 2701.
(84) Balsara, N. P.; Stepanek, P.; Lodge, T. P.; Tirrell, M. *Macromolecules* **1991**, *24*, 6227.
(85) Ngai, K. L. *Adv. Colloid Interface Sci*. **1996**, *64*, 1.
(86) Ngai, K. L.; Phillies, G. D. J. *J. Chem. Phys.* **1996**, *105*, 8385.
(87) Annable, T.; Buscall, R.; Ettelaie, R.; Whittlestone, D. *J. Rheol.* **1993**, *37*, 695.
(88) Walderhaug, H.; Hansen, F. K.; Abrahmsén, S., Persson, K.; Stilbs, P. *J. Phys. Chem.* **1993**, *97*, 8336.
(89) Huldén, M. *Colloids Surf., A* **1994**, *82*, 263.
(90) Tam, K. C.; Jenkins, R. D.; Winnik, M. A.; Bassett, D. R. *Macromolecules* **1998**, *31*, 4149.
(91) Butler, G. B.; O′Driscoll, K. F.; Wilkes, G. L. *J. Macromol. Sci., Rev. Macromol. Chem. Phys.* **1988**, *C28*, 1.
(92) Nyström, B.; Walderhaug, H. *J. Phys. Chem.* **1996**, *100*, 5433.
(93) Kopperud, H. M.; Hansen, F. K.; Nyström, B. *Macromol. Chem. Phys.* **1998**, *199*, 2385.
(94) Nguyen-Misra, M.; Mattice, W. L. *Macromolecules* **1995**, *28*, 6976.
(95) Lairez, D.; Adam, M.; Raspaud, E.; Carton, J.-P.; Bouchaud, J.-P. *Macromol. Symp.* **1995**, *90*, 203.
(96) Raspaud, E.; Lairez, D.; Adam, M.; Carton, J.-P. *Macromolecules* **1996**, *29*, 1269.